

Kaon Production and Kaon to Pion Ratio in Au+Au Collisions at $\sqrt{s_{NN}} = 130$ GeV

C. Adler¹¹, Z. Ahammed²³, C. Allgower¹², J. Amonett¹⁴, B.D. Anderson¹⁴, M. Anderson⁵, G.S. Averichev⁹, J. Balewski¹², O. Barannikova^{9,23}, L.S. Barnby¹⁴, J. Baudot¹³, S. Bekele²⁰, V.V. Belaga⁹, R. Bellwied³¹, J. Berger¹¹, H. Bichsel³⁰, A. Billmeier³¹, L.C. Bland², C.O. Blyth³, B.E. Bonner²⁴, A. Boucham²⁶, A. Brandin¹⁸, A. Bravar², R.V. Cadman¹, H. Caines³³, M. Calderón de la Barca Sánchez², A. Cardenas²³, J. Carroll¹⁵, J. Castillo²⁶, M. Castro³¹, D. Cebra⁵, P. Chaloupka²⁰, S. Chattopadhyay³¹, Y. Chen⁶, S.P. Chernenko⁹, M. Cherney⁸, A. Chikanian³³, B. Choi²⁸, W. Christie², J.P. Coffin¹³, T.M. Cormier³¹, J.G. Cramer³⁰, H.J. Crawford⁴, W.S. Deng², A.A. Derevschikov²², L. Didenko², T. Dietel¹¹, J.E. Draper⁵, V.B. Dunin⁹, J.C. Dunlop³³, V. Eckardt¹⁶, L.G. Efimov⁹, V. Emelianov¹⁸, J. Engelage⁴, G. Eppley²⁴, B. Erasmus²⁶, P. Fachini², V. Faine², J. Faivre¹³, K. Filimonov¹⁵, E. Finch³³, Y. Fisyak², D. Flierl¹¹, K.J. Foley², J. Fu^{15,32}, C.A. Gagliardi²⁷, N. Gagunashvili⁹, J. Gans³³, L. Gaudichet²⁶, M. Germain¹³, F. Geurts²⁴, V. Ghazikhanian⁶, O. Grachov³¹, V. Grigoriev¹⁸, M. Guedon¹³, E. Gushin¹⁸, T.J. Hallman², D. Hardtke¹⁵, J.W. Harris³³, T.W. Henry²⁷, S. Heppelmann²¹, T. Herston²³, B. Hippolyte¹³, A. Hirsch²³, E. Hjort¹⁵, G.W. Hoffmann²⁸, M. Horsley³³, H.Z. Huang⁶, T.J. Humanic²⁰, G. Igo⁶, A. Ishihara²⁸, Yu.I. Ivanshin¹⁰, P. Jacobs¹⁵, W.W. Jacobs¹², M. Janik²⁹, I. Johnson¹⁵, P.G. Jones³, E.G. Judd⁴, M. Kaneta¹⁵, M. Kaplan⁷, D. Keane¹⁴, J. Kiryluk⁶, A. Kisiel²⁹, J. Klay¹⁵, S.R. Klein¹⁵, A. Klyachko¹², A.S. Konstantinov²², M. Kopytine¹⁴, L. Kotchenda¹⁸, A.D. Kovalenko⁹, M. Kramer¹⁹, P. Kravtsov¹⁸, K. Krueger¹, C. Kuhn¹³, A.I. Kulikov⁹, G.J. Kunde³³, C.L. Kunz⁷, R.Kh. Kutuev¹⁰, A.A. Kuznetsov⁹, L. Lakehal-Ayat²⁶, M.A.C. Lamont³, J.M. Landgraf², S. Lange¹¹, C.P. Lansdel²⁸, B. Lasiuk³³, F. Laue², J. Lauret², A. Lebedev², R. Lednický⁹, V.M. Leontiev²², M.J. LeVine², Q. Li³¹, S.J. Lindenbaum¹⁹, M.A. Lisa²⁰, F. Liu³², L. Liu³², Z. Liu³², Q.J. Liu³⁰, T. Ljubicic², W.J. Llope²⁴, G. LoCurto¹⁶, H. Long⁶, R.S. Longacre², M. Lopez-Noriega²⁰, W.A. Love², T. Ludlam², D. Lynn², J. Ma⁶, R. Majka³³, S. Margetis¹⁴, C. Markert³³, L. Martin²⁶, J. Marx¹⁵, H.S. Matis¹⁵, Yu.A. Matulenko²², T.S. McShane⁸, F. Meissner¹⁵, Yu. Melnick²², A. Meschanin²², M. Messer², M.L. Miller³³, Z. Milosevich⁷, N.G. Minaev²², J. Mitchell²⁴, V.A. Moiseenko¹⁰, C.F. Moore²⁸, V. Morozov¹⁵, M.M. de Moura³¹, M.G. Munhoz²⁵, J.M. Nelson³, P. Nevski², V.A. Nikitin¹⁰, L.V. Nogach²², B. Norman¹⁴, S.B. Nurushev²², G. Odyniec¹⁵, A. Ogawa²¹, V. Okorokov¹⁸, M. Oldenburg¹⁶, D. Olson¹⁵, G. Paic²⁰, S.U. Pandey³¹, Y. Panebratsev⁹, S.Y. Panitkin², A.I. Pavlinov³¹, T. Pawlak²⁹, V. Perevoztchikov², W. Peryt²⁹, V.A. Petrov¹⁰, M. Planinic¹², J. Pluta²⁹, N. Porile²³, J. Porter², A.M. Poskanzer¹⁵, E. Potrebenikova⁹, D. Prindle³⁰, C. Pruneau³¹, J. Putschke¹⁶, G. Rai¹⁵, G. Rakness¹², O. Ravel²⁶, R.L. Ray²⁸, S.V. Razin^{9,12}, D. Reichhold⁸, J.G. Reid³⁰, G. Renault²⁶, F. Retiere¹⁵, A. Ridiger¹⁸, H.G. Ritter¹⁵, J.B. Roberts²⁴, O.V. Rogachevski⁹, J.L. Romero⁵, A. Rose³¹, C. Roy²⁶, V. Rykov³¹, I. Sakrejda¹⁵, S. Salur³³, J. Sandweiss³³, A.C. Saulys², I. Savin¹⁰, J. Schambach²⁸, R.P. Scharenberg²³, N. Schmitz¹⁶, L.S. Schroeder¹⁵, A. Schüttauf¹⁶, K. Schweda¹⁵, J. Seger⁸, D. Seliverstov¹⁸, P. Seyboth¹⁶, E. Shahaliev⁹, K.E. Shestermanov²², S.S. Shimanski⁹, V.S. Shvetcov¹⁰, G. Skoro⁹, N. Smirnov³³, R. Snellings¹⁵, P. Sorensen⁶, J. Sowinski¹², H.M. Spinka¹, B. Srivastava²³, E.J. Stephenson¹², R. Stock¹¹, A. Stolpovsky³¹, M. Strikhanov¹⁸, B. Stringfellow²³, C. Struck¹¹, A.A.P. Suaide³¹, E. Sugarbaker²⁰, C. Suire², M. Šumbera²⁰, B. Surrow², T.J.M. Symons¹⁵, A. Szanto de Toledo²⁵, P. Szarwas²⁹, A. Tai⁶, J. Takahashi²⁵, A.H. Tang¹⁵, J.H. Thomas¹⁵, M. Thompson³, V. Tikhomirov¹⁸, M. Tokarev⁹, M.B. Tonjes¹⁷, T.A. Trainor³⁰, S. Trentalange⁶, R.E. Tribble²⁷, V. Trofimov¹⁸, O. Tsai⁶, T. Ullrich², D.G. Underwood¹, G. Van Buren², A.M. VanderMolen¹⁷, I.M. Vasilevski¹⁰, A.N. Vasiliev²², S.E. Vigdor¹², S.A. Voloshin³¹, F. Wang²³, H. Ward²⁸, J.W. Watson¹⁴, R. Wells²⁰, G.D. Westfall¹⁷, C. Whitten Jr.⁶, H. Wieman¹⁵, R. Willson²⁰, S.W. Wissink¹², R. Witt³³, J. Wood⁶, N. Xu¹⁵, Z. Xu², A.E. Yakutin²², E. Yamamoto¹⁵, J. Yang⁶, P. Yepes²⁴, V.I. Yurevich⁹, Y.V. Zanevski⁹, I. Zborovský⁹, H. Zhang³³, W.M. Zhang¹⁴, R. Zoukarneev¹⁰, A.N. Zubarev⁹

(STAR Collaboration)

¹Argonne National Laboratory, Argonne, Illinois 60439

²Brookhaven National Laboratory, Upton, New York 11973

³University of Birmingham, Birmingham, United Kingdom

⁴University of California, Berkeley, California 94720

⁵University of California, Davis, California 95616

⁶University of California, Los Angeles, California 90095

⁷Carnegie Mellon University, Pittsburgh, Pennsylvania 15213

⁸Creighton University, Omaha, Nebraska 68178

⁹Laboratory for High Energy (JINR), Dubna, Russia

¹⁰Particle Physics Laboratory (JINR), Dubna, Russia

¹¹University of Frankfurt, Frankfurt, Germany

- ¹²Indiana University, Bloomington, Indiana 47408
¹³Institut de Recherches Subatomiques, Strasbourg, France
¹⁴Kent State University, Kent, Ohio 44242
¹⁵Lawrence Berkeley National Laboratory, Berkeley, California 94720
¹⁶Max-Planck-Institut fuer Physik, Munich, Germany
¹⁷Michigan State University, East Lansing, Michigan 48824
¹⁸Moscow Engineering Physics Institute, Moscow Russia
¹⁹City College of New York, New York City, New York 10031
²⁰Ohio State University, Columbus, Ohio 43210
²¹Pennsylvania State University, University Park, Pennsylvania 16802
²²Institute of High Energy Physics, Protvino, Russia
²³Purdue University, West Lafayette, Indiana 47907
²⁴Rice University, Houston, Texas 77251
²⁵Universidade de Sao Paulo, Sao Paulo, Brazil
²⁶SUBATECH, Nantes, France
²⁷Texas A&M University, College Station, Texas 77843
²⁸University of Texas, Austin, Texas 78712
²⁹Warsaw University of Technology, Warsaw, Poland
³⁰University of Washington, Seattle, Washington 98195
³¹Wayne State University, Detroit, Michigan 48201
³²Institute of Particle Physics, CCNU (HZNU), Wuhan, 430079 China and
³³Yale University, New Haven, Connecticut 06520

Mid-rapidity transverse mass spectra and multiplicity densities of charged and neutral kaons are reported for Au+Au collisions at $\sqrt{s_{NN}}=130$ GeV at RHIC. The spectra are exponential in transverse mass, with an inverse slope of about 280 MeV in central collisions. The multiplicity densities for these particles scale with the negative hadron pseudo-rapidity density. The charged kaon to pion ratios are $K^+/\pi^- = 0.161 \pm 0.002(\text{stat}) \pm 0.024(\text{syst})$ and $K^-/\pi^- = 0.146 \pm 0.002(\text{stat}) \pm 0.022(\text{syst})$ for the most central collisions. The K^+/π^- ratio is lower than the same ratio observed at the SPS while the K^-/π^- is higher than the SPS result. Both ratios are enhanced by about 50% relative to p+p and \bar{p} +p collision data at similar energies.

PACS numbers: 25.75.-q, 25.75.Dw

Lattice QCD predicts that at sufficiently high energy density, matter will be in a state of deconfined quarks and gluons [1]. It has been suggested that strangeness production is a sensitive probe of a deconfined state: for example, strangeness production may be enhanced by the fast and energetically favorable process of gluon-gluon fusion into strange quark-antiquark pairs [2]. Hadronic mechanisms, on the other hand, may also enhance strangeness production [3]. A systematic investigation of strangeness production is therefore needed to understand different production mechanisms.

Strangeness production has been studied in heavy-ion collisions at the AGS [4, 5, 6], SPS [7, 8, 9], and more recently at RHIC [10, 11, 12]. In this letter, we report measurements by the STAR experiment at RHIC on charged and neutral kaon production. The measurements were made at mid-rapidity in Au+Au collisions at a nucleon-nucleon center-of-mass energy of $\sqrt{s_{NN}}=130$ GeV. The measurements were carried out during the summer of 2000 and details of the STAR experiment are described elsewhere [13, 14, 15]. The primary tracking device in the experiment is a Time Projection Chamber (TPC). It sits in a magnetic field of 0.25 Tesla. Tracks were reconstructed from three-dimensional hits measured in the TPC and the primary vertex of the interaction was found

by fitting the reconstructed tracks to a common point of origin. Corrections were made for the energy loss of the charged kaons in the detector material. The momentum resolution was found to have negligible effect on the kaon spectra and so no correction was applied.

Two methods were used to identify the kaons:

(I) The Energy loss method (dE/dx): Particle identification was done by measuring the mean specific energy lost by the charged particles, $\langle dE/dx \rangle$, in the TPC gas. The $\langle dE/dx \rangle$ resolution was approximately 11%. The tracks were required to come from within 3 cm of the primary vertex and every track had at least 25 hits, out of 45 possible hits, on the TPC pad plane. Using a method that is described in [15], the distribution in $\ln[\langle dE/dx \rangle / \langle dE/dx \rangle_{\text{BB}}]$ (where $\langle dE/dx \rangle_{\text{BB}}$ is the expected Bethe-Bloch value) was fit by a sum of four Gaussians corresponding to π^\pm , K^\pm , e^\pm , and p (\bar{p}). The fit was done for each centrality and transverse momentum (p_\perp) bin. The raw kaon yield was extracted from the fit parameters. In the range where the kaons are well separated from other species, $p_\perp \lesssim 0.5$ GeV/c, we estimate a point-to-point systematic error of 5% on the extracted kaon yields. In the range where the kaons and the e^\pm overlap in $\langle dE/dx \rangle$, $0.5 \lesssim p_\perp \lesssim 0.7$ GeV/c, we parameterized the e^\pm yield using data from lower p_\perp and

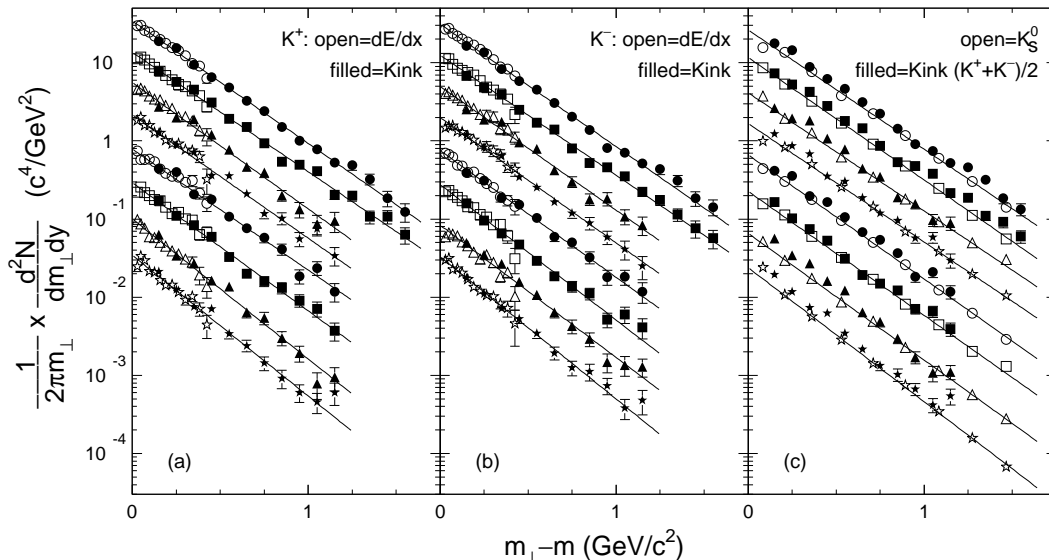


FIG. 1: Invariant yields for K^+ , K^- and K_S^0 versus m_\perp . In figure (a) K^+ and (b) K^- , the kaons are identified by the dE/dx method ($|y| < 0.1$) and by the *Kink* method ($|y| < 0.5$). In figure (c) the K_S^0 is identified by the K_S^0 method ($|y| < 0.5$) and the $(K^+ + K^-)/2$ is from the *Kink* analysis. The data are plotted in order of decreasing centrality from top to bottom. See Table I. The most central collision spectrum is shown full scale; the other spectra are divided by 2,4,8,16,32,64, and 64 for display purposes. The error bars are uncorrelated random errors. See text for a description of the systematic errors. The solid lines are m_\perp exponential fits to the K^+ , K^- , and K_S^0 spectra, respectively.

Monte Carlo (MC) simulations and estimate the systematic errors to range from 10% to 20%. In the region where the kaons significantly merge with the pions in $\langle dE/dx \rangle$, $0.7 \lesssim p_\perp \lesssim 0.8$ GeV/c, we neglect the e^\pm contribution and estimate the systematic errors to be on the order of 15% [16].

(II) The Decay topology method (*Kink* and K_S^0): Charged kaons can be identified topologically via their one-prong, ‘kink’, decays (e.g. $K \rightarrow \mu\nu$, $K \rightarrow \pi\pi^0$) [17, 18]. The parent kaon and charged daughter tracks are used to determine the decay kinematics. The decay position was restricted by a fiducial cut inside the volume of the TPC to improve the signal to background ratio. Background sources include charged pion decays, hadronic interactions in the TPC gas, and combinatorics. A momentum dependent decay angle cut was used to eliminate essentially all pion decays because they have a much smaller decay angle. A remaining background of the order of 15% is corrected for in the kaon spectra [18].

Neutral kaons were reconstructed via their decay $K_S^0 \rightarrow \pi^+\pi^-$. A pair of oppositely charged tracks formed a K_S^0 decay-candidate if their distance of closest approach to each other was less than 1 cm. The majority of the combinatorial background was eliminated by requiring that the daughter tracks miss the primary vertex by at least 1.5 cm, and the decay vertex had to be separated from the primary vertex by more than 6 cm [19]. A cut on the $\langle dE/dx \rangle$ of the daughters was also applied to remove a majority of the contribution from $\Lambda \rightarrow p\pi^-$ and $\bar{\Lambda} \rightarrow \bar{p}\pi^+$ decays.

In all cases, the primary vertex was restricted to a

limited longitudinal range near the center of the TPC. The event centrality was determined off-line and is based on measured charged particle multiplicities in the TPC. A correction factor was applied to account for losses due to limited acceptance, decay, tracking inefficiency, and hadronic interactions. The overall efficiency (ϵ), including all these effects, was obtained from a full MC simulation by embedding MC tracks into real events on the raw data level. For the most central collisions, the dE/dx method yielded $\epsilon \simeq 20\%$ at $p_\perp=0.2$ GeV/c and 60% at 0.7 GeV/c. For the *Kink* method, $\epsilon \simeq 1.5\%$ at $p_\perp=1$ GeV/c and 0.6% at 2 GeV/c. For the K_S^0 method, $\epsilon \simeq 4.5\%$ at $p_\perp=1$ GeV/c and 7% at 2 GeV/c. The efficiency increases with decreasing event multiplicity by about 20% of its value, from the most central to the most peripheral bins, for the dE/dx and *Kink* methods and by 70% for the K_S^0 method.

Figure 1 shows the transverse mass spectra for the invariant yields of K^+ , K^- , and K_S^0 , where $m_\perp \equiv \sqrt{p_\perp^2 + m^2}$ and m is the kaon mass. The errors shown for the dE/dx method are the quadratic sum of the statistical and point-to-point systematic errors. The errors shown for *Kink* and K_S^0 methods are statistical only. The overall systematic errors are estimated to be 5%, 10%, and 10% for dE/dx , *Kink*, and K_S^0 methods, respectively; they are uncorrelated among the three analyses. An additional 5% systematic error, due to uncertainties in our MC determination of the efficiencies, applies to all three analyses. Figure 1(c) compares K_S^0 spectra to the averaged charged kaon spectra from the *Kink* method. As isospin asymmetry is negligible at mid-rapidity [20], the

TABLE I: The mid-rapidity kaon multiplicity densities (dN/dy) and m_{\perp} exponential inverse slopes (T in MeV) as a function of negative hadron multiplicity within $|\eta| < 0.5$ ($dN_{h^-}/d\eta$). Quoted errors are uncorrelated errors (first) and correlated systematic errors (second). See text for details. Systematic error on $dN_{h^-}/d\eta$ is 7%. The centrality bins are as same as in Ref. [15].

Centrality bin	$\frac{dN_{h^-}}{d\eta}$	K^+		K^-		K_S^0	
		dN/dy	T	dN/dy	T	dN/dy	T
58-85%	17.9	$2.46 \pm 0.07 \pm 0.32$	$241 \pm 7 \pm 19$	$2.32 \pm 0.06 \pm 0.30$	$238 \pm 7 \pm 19$	$1.82 \pm 0.04 \pm 0.27$	$253 \pm 4 \pm 15$
45-58%	47.3	$7.23 \pm 0.18 \pm 0.95$	$242 \pm 6 \pm 19$	$6.48 \pm 0.17 \pm 0.84$	$257 \pm 7 \pm 21$	$5.40 \pm 0.10 \pm 0.81$	$268 \pm 3 \pm 16$
34-45%	78.9	$11.8 \pm 0.3 \pm 1.5$	$265 \pm 6 \pm 21$	$10.4 \pm 0.2 \pm 1.4$	$250 \pm 6 \pm 20$	$9.57 \pm 0.17 \pm 1.4$	$274 \pm 3 \pm 16$
26-34%	115.	$17.2 \pm 0.4 \pm 2.3$	$281 \pm 7 \pm 22$	$15.5 \pm 0.4 \pm 2.0$	$268 \pm 7 \pm 21$	$14.0 \pm 0.2 \pm 2.1$	$273 \pm 3 \pm 16$
18-26%	154.	$23.1 \pm 0.5 \pm 3.0$	$275 \pm 7 \pm 22$	$20.8 \pm 0.5 \pm 2.7$	$271 \pm 7 \pm 22$	$18.8 \pm 0.3 \pm 2.8$	$287 \pm 3 \pm 17$
11-18%	196.	$28.8 \pm 0.7 \pm 3.8$	$269 \pm 6 \pm 22$	$26.4 \pm 0.6 \pm 3.4$	$274 \pm 7 \pm 22$	$23.3 \pm 0.4 \pm 3.5$	$287 \pm 3 \pm 17$
6-11%	236.	$38.0 \pm 0.6 \pm 5.0$	$284 \pm 4 \pm 23$	$34.5 \pm 0.5 \pm 4.5$	$283 \pm 4 \pm 23$	$31.4 \pm 0.5 \pm 4.7$	$277 \pm 3 \pm 17$
0-6%	290.	$46.2 \pm 0.6 \pm 6.1$	$277 \pm 4 \pm 22$	$41.9 \pm 0.6 \pm 5.4$	$277 \pm 4 \pm 22$	$36.7 \pm 0.6 \pm 5.5$	$285 \pm 3 \pm 17$

primordial K_S^0 yield is most likely equal to the average of the primordial charged kaon yields. However, our measurements include decay products of ϕ mesons which decay into charged kaons and neutral kaons with different branching ratios. The effect is estimated using the measured ϕ spectra [10] to be 1-3% between the measured charged and neutral kaons in the $0.2 < p_{\perp} < 1.0$ GeV/ c range.

The kaon spectra exhibit an exponential shape in m_{\perp} . We fit the spectra of charged kaons (combined from dE/dx and *Kink*) and K_S^0 , respectively, to an m_{\perp} exponential with the inverse slope, T , and the integrated rapidity density, dN/dy , as free parameters. The fit results are shown as solid lines in Fig. 1. The fit parameters are listed in Table I together with $dN_{h^-}/d\eta$, the negative hadron multiplicity within $|\eta| < 0.5$ [14]. Systematic errors on dN/dy and T are both about 8% for charged kaons, and 10% and 6%, respectively, for K_S^0 . The systematic errors are partially correlated between K^+ and K^- . An additional 5% systematic error applies to the dN/dy and it is correlated between all three particle species. Our charged kaon dN/dy results are in agreement with the recent PHENIX publication [11] and the point-by-point spectra agree within two standard deviation of systematic errors.

Figure 2(a) shows T as a function of $dN_{h^-}/d\eta$. No difference is observed between the K^+ , K^- and K_S^0 . There is an indication of a systematic increase in T from ~ 240 MeV in the most peripheral collisions to ~ 280 MeV in the most central collisions. For comparison, the kaon inverse slope is about 240 MeV for central heavy ion collisions at the SPS ($\sqrt{s_{NN}} \approx 17$ GeV) [8, 9, 21] and 200 MeV at the AGS ($\sqrt{s_{NN}} \approx 5$ GeV) [5, 6]. Note, however, that inverse slopes may measure a combined effect of thermal temperature and transverse radial flow [21] and the larger T values suggest stronger radial flow at RHIC energies. For the most central collisions, the measured kaon T is smaller than that of the lambda and the lambda dN/dy [12] is about 1/3 of the kaon dN/dy . As a result,

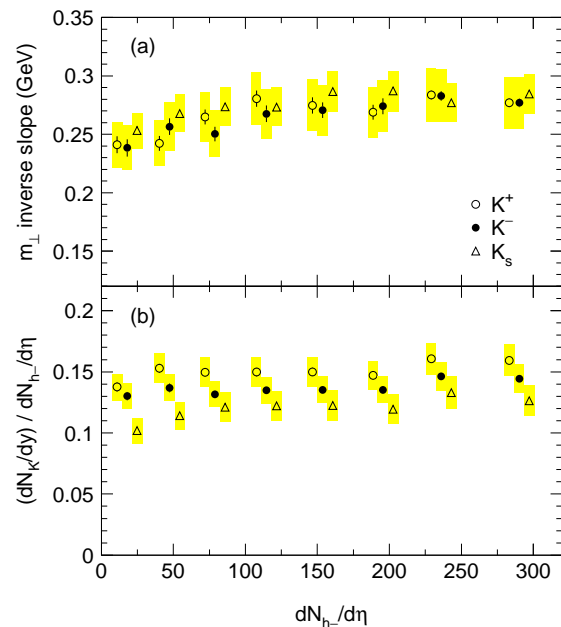


FIG. 2: The centrality dependence of (a) kaon inverse slopes and (b) mid-rapidity kaon to negative hadron ratios. The error bars are uncorrelated random errors; correlated systematic errors are indicated by the shaded areas. An additional systematic error (not shown) of 5% and 7% applies to the dN/dy of kaons and $dN_{h^-}/d\eta$, respectively. For clarity the K^+ and K_S^0 points are displaced in $dN_{h^-}/d\eta$.

the lambda yield approaches, and may even exceed the kaon yield for $p_{\perp} \gtrsim 1.5$ GeV/ c . A similar behaviour was observed for non-strange particles (pion and proton) in a similar p_{\perp} region [11].

Figure 2(b) shows the ratio of kaon dN/dy to $dN_{h^-}/d\eta$ as a function of $dN_{h^-}/d\eta$. No strong centrality dependence is observed for the ratios, suggesting no significant change in strangeness production mechanisms from peripheral to central collisions at this RHIC energy. In contrast, kaon production at lower AGS and SPS energies roughly doubles from peripheral to central colli-

sions [5, 8]. On the other hand, the K^+/K^- ratio remains constant as a function of centrality at all energies [5, 8, 22].

K/π ratios are often used to study strangeness production enhancement. In order to evaluate K/π , we deduce the mid-rapidity pion dN_{π^-}/dy in central collisions from our measurements of negative hadrons [14], antiprotons [15] and K^- spectra. The deduced mid-rapidity value is $dN_{\pi^-}/dy = 287 \pm 20$, consistent with our preliminary measurement of pion spectra cited in [23]. For the most central collisions, $K^+/\pi^- = 0.161 \pm 0.002(\text{stat}) \pm 0.024(\text{syst})$ and $K^-/\pi^- = 0.146 \pm 0.002(\text{stat}) \pm 0.022(\text{syst})$. The systematic errors are a quadratic sum of those on the kaon and the pion dN/dy . Figure 3 is a compilation of K/π results for central heavy ion collisions. Since mid-rapidity $\pi^+/\pi^- \approx 1$ at RHIC [20], we can readily compare our K^+/π^- results to K^+/π^+ results from lower energies. The K^-/π ratio steadily increases with $\sqrt{s_{\text{NN}}}$, while the K^+/π ratio in heavy ion collisions sharply increases at low energies and the maximum value of K^+/π^+ occurs at $\sqrt{s_{\text{NN}}} \sim 10$ GeV. This value is determined by the interplay between the dropping net-baryon density with $\sqrt{s_{\text{NN}}}$ and an increasing $K\bar{K}$ pair production rate, as previously noted (e.g. in [22, 24]).

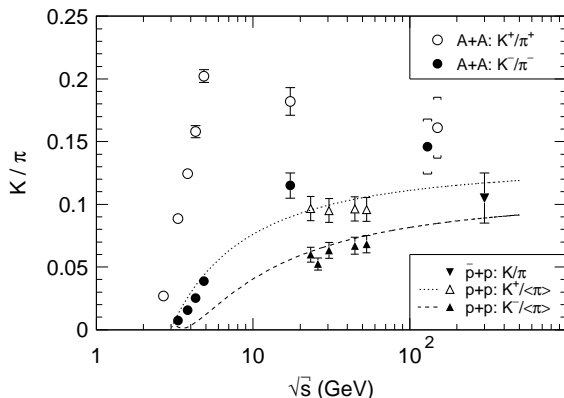


FIG. 3: Mid-rapidity K/π ratios versus $\sqrt{s_{\text{NN}}}$. The curves are parameterizations to p+p data [25]. The error bars show statistical errors. The systematic errors on the STAR data are indicated by the caps. The STAR K^+/π^+ point is displaced in $\sqrt{s_{\text{NN}}}$ for clarity.

Figure 3 also shows parameterized p+p data (curves) and data from p+p [25] and $\bar{p}+p$ [26] at higher energies. Our measurement indicates a 50% enhancement over $(K^+ + K^-)/2\langle\pi\rangle$ in p+p and $\bar{p}+p$ collisions at similar energies. The enhancement in K^-/π is similar at SPS and RHIC, while that in K^+/π is larger at lower energies due to the effect of a changing net-baryon density.

In conclusion, we have reported invariant yield transverse mass spectra and multiplicity densities of charged and neutral kaons at mid-rapidity in Au+Au collisions at $\sqrt{s_{\text{NN}}}=130$ GeV at RHIC. The spectra are described

by an exponential in transverse mass. The inverse slope parameters are found to increase slightly with collision centrality, with a value of about 280 MeV in central collisions. No strong centrality dependence is found in the ratio of kaon densities to negative hadron pseudo-rapidity densities. For the most central collisions, the mid-rapidity kaon to pion ratios are $K^+/\pi^- = 0.161 \pm 0.002(\text{stat}) \pm 0.024(\text{syst})$ and $K^-/\pi^- = 0.146 \pm 0.002(\text{stat}) \pm 0.022(\text{syst})$. For central heavy ion collisions, the K^+/π ratio is found to increase rapidly with the collision energy and then to decrease, while the K^-/π ratio increases steadily. This behavior is consistent with the increasing pair production rate as the collision energy increases, and the decreasing net-baryon density at mid-rapidity. The measured K/π ratios at RHIC show an enhancement of about 50% over p+p and $\bar{p}+p$ collisions at similar energies.

We wish to thank the RHIC Operations Group and the RHIC Computing Facility at Brookhaven National Laboratory, and the National Energy Research Scientific Computing Center at Lawrence Berkeley National Laboratory for their support. This work was supported by the Division of Nuclear Physics and the Division of High Energy Physics of the Office of Science of the U.S. Department of Energy, the United States National Science Foundation, the Bundesministerium fuer Bildung und Forschung of Germany, the Institut National de la Physique Nucleaire et de la Physique des Particules of France, the United Kingdom Engineering and Physical Sciences Research Council, Fundacao de Amparo a Pesquisa do Estado de Sao Paulo, Brazil, and the Russian Ministry of Science and Technology.

- [1] E. Laermann, Nucl. Phys. **A610**, 1c (1996).
- [2] J. Rafelski and B. Müller, Phys. Rev. Lett. **48**, 1066 (1982); *ibid* **56**, 2334(E) (1986); J. Rafelski, Phys. Rep. **88**, 331 (1982); R. Koch, B. Müller, and J. Rafelski, Phys. Rep. **142**, 167 (1986).
- [3] H. Sorge *et al.*, Phys. Lett. B **271**, 37 (1991); H. Sorge, Phys. Rev. C **52** (1995) 3291.
- [4] T. Abbott *et al.* (E802 Collab.), Phys. Rev. Lett. **66**, 1567 (1991); Phys. Rev. D **45**, 3906 (1992); Phys. Rev. C **50**, 1024 (1994).
- [5] L. Ahle *et al.* (E802 Collab.), Phys. Rev. C **60**, 044904 (1999); *ibid* **58**, 3523 (1998); *ibid* **57**, 466 (1998); F. Wang (E802 Collab.), in Proc. of Heavy-Ion Physics at the AGS, WSU-NP-96-16 (1996).
- [6] L. Ahle *et al.* (E866 Collab.) and B.B. Back *et al.* (E917 Collab.), Phys. Lett. B **476**, 1 (2000); *ibid* **490**, 53 (2000).
- [7] J. Bartke *et al.* (NA35 Collab.), Z. Phys. **C48**, 191 (1990); T. Alber *et al.* (NA35 Collab.), Eur. Phys. J. C **2**, 643 (1998).
- [8] F. Siklér (NA49 Collab.), Nucl. Phys. **A661**, 45c (1999); C. Höhne (NA49 Collab.), Nucl. Phys. **A661**, 485c (1999).
- [9] I.G. Bearden *et al.* (NA44 Collab.), Phys. Lett. **B471**,

- 6 (1999); H. Bøggild *et al.* (NA44 Collab.), Phys. Rev. C **59**, 328 (1999); I.G. Bearden *et al.* (NA44 Collab.), nucl-ex/0202019.
- [10] C. Adler *et al.* (STAR Collab.), Phys. Rev. C **65**, 041901R (2002).
- [11] K. Adcox *et al.* (PHENIX Collab.), Phys. Rev. Lett. **88**, 242301 (2002).
- [12] C. Adler *et al.* (STAR Collab.), accepted to Phys. Rev. Lett. [nucl-ex/0203016].
- [13] K.H. Ackermann *et al.* (STAR Collab.), Nucl. Phys. **A661**, 681c (1999); Phys. Rev. Lett. **86**, 402 (2001); C. Adler *et al.* (STAR Collab.), Phys. Rev. Lett. **86**, 4778 (2001).
- [14] C. Adler *et al.* (STAR Collab.), Phys. Rev. Lett. **87**, 112303 (2001).
- [15] C. Adler *et al.* (STAR Collab.), Phys. Rev. Lett. **87**, 262302 (2001).
- [16] A. Cardenas, Ph.D. thesis, Purdue University, 2002.
- [17] S. Margetis, K. Safarik, and O. Villalobos Baillie, Ann. Rev. Nucl. Part. Sci. **50**, 299 (2000).
- [18] W. Deng, Ph.D. thesis, Kent State University, 2002.
- [19] M.A.C. Lamont, Ph.D. thesis, Univeristy of Birmingham, 2002.
- [20] B.B. Back *et al.* (PHOBOS Collab.), Phys. Rev. Lett. **87**, 102301 (2001).
- [21] I. G. Bearden *et al.* (NA44 Collab.), Phys. Rev. Lett. **78**, 2080 (1997); N. Xu and M. Kaneta, Nucl. Phys. **A698**, 306c (2002).
- [22] F. Wang, Phys. Lett. B **489**, 273 (2000).
- [23] J.W. Harris (STAR Collab.), Nucl. Phys. **A698**, 64c (2002); M. Calderón de la Barca Sánchez, Ph.D. thesis, Yale University, 2001 [nucl-ex/0111004].
- [24] F. Wang *et al.*, Phys. Rev. C **61**, 064904 (2000); F. Wang and N. Xu, Phys. Rev. C. **61**, 021904 (2000); J.C. Dunlop and C.A. Ogilvie, Phys. Rev. C **61**, 031901 (2000); P. Braun-Munzinger *et al.*, Nucl. Phys. **A697**, 902 (2002).
- [25] A.M. Rossi *et al.*, Nucl. Phys. B **84**, 269 (1975); J.L. Bailly *et al.* (NA23 Collab.), Phys. Lett. B **195**, 609 (1987).
- [26] T. Alexopoulos *et al.*, Phys. Rev. D **48**, 984 (1993).